

Reaction Mechanisms

Powerful Insight into Catalytic Mechanisms through Simultaneous Monitoring of Reactants, Products, and Intermediates**

Krista L. Vikse, Zohrab Ahmadi, Cara C. Manning, David A. Harrington, and J. Scott McIndoe*

Electrospray ionization mass spectrometry (ESIMS) has become a valuable tool in the mechanistic study of organometallic catalytic reactions. Analysis is fast, intermediates at low concentrations can be detected, and complex mixtures are tractable. The family of palladium-catalyzed C–C bond-forming reactions are the most studied by ESIMS.^[1–14] Although the majority of these investigations have focused on the structural identification of short-lived or low-concentration intermediates, some recent studies have monitored the intensities of intermediates or reactants and products over time.^[5,14] However, no one has yet shown this technique to be capable of providing robust kinetic information for reactants, products, by-products, and low-abundance intermediates simultaneously and under standard reaction conditions. We show herein how powerful this information can be in leading reaction design.

The copper-free Sonogashira (Heck alkynylation) reaction is widely used in the synthesis of natural products, pharmaceuticals, and novel materials, but the mechanism is not well understood.^[15] Ideally, the reaction should be observed under typical reaction conditions for meaningful information to be obtained about the mechanism, because under such conditions anions^[16] and bases^[17,18] as well as alkynes^[19] are thought to act as ligands for palladium, with complex effects on the reaction efficiency.

In most cases, a large excess of an amine base is required to promote reaction; however, the exact role of the base is in question.^[15] Dieck and Heck^[20] and Amatore et al.^[21] suggested a carbopalladation mechanism in which the terminal alkyne undergoes carbopalladation and the base consumes the H⁺ formed during the β-hydride elimination that forms the product. Ljundahl et al.^[22] prefer a deprotonation mechanism in which deprotonation of the terminal alkyne by the amine occurs from the cationic intermediate [Pd(Ar)(PR₃)(NR'₂)(HC≡CR'')] or the neutral intermediate [Pd(Ar)(PR₃)(X)(HC≡CR'')], depending on the electronic nature of the alkyne. An anionic mechanism has also been proposed in which [Pd⁰(PR₃)₂X][−] and [Pd^{II}(PR₃)(X)(Ar)(CCR'')][−] inter-

mediates feature.^[16] The identity of palladium-containing intermediates has been proposed on the basis of electrochemical or NMR spectroscopic data but not through direct observation.

Charged tags are required for the detection of species otherwise invisible to ESIMS,^[23,24] an idea first introduced by Adlhart and Chen;^[25] we used an aryl iodide functionalized with a phosphonium hexafluorophosphate salt, [p-IC₆H₄-CH₂PPh₃]⁺[PF₆][−]. This tag provides very low detection limits owing to its high surface activity, and the noncoordinating counterion reduces ion pairing. The bulky nature of the charged group ensures that the ionization efficiency is largely insensitive to the remaining structure of the ion, so the intensity of the various ions correspond very closely to their real concentration (see the Supporting Information). ESIMS data on reaction progress collected under typical reaction conditions by using pressurized sample infusion (PSI)^[26] compare well with ¹H NMR and UV/Vis spectroscopic data (Figure 1). The number of data points is much higher for

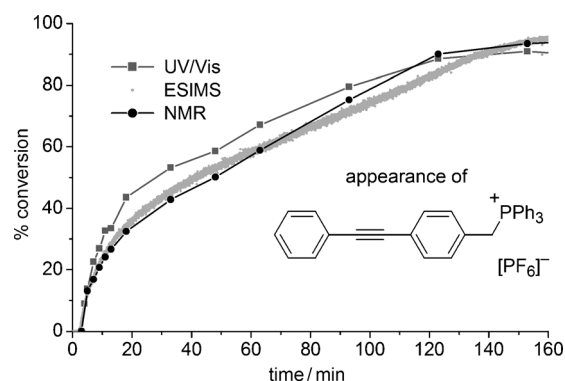


Figure 1. Appearance of the product (ArC₂Ph), as tracked by three different techniques: ¹H NMR spectroscopy, UV/Vis spectroscopy, and ESIMS.

ESIMS because the reaction is monitored continuously at 1 spectrum per second, whereas the other techniques require a more conventional periodic sample–quench–concentrate–analyze approach.

The intensities of all tagged species observed during a typical reaction appear in Figure 2. The relative concentrations of the product (ArC₂Ph), substrate (ArI), and by-product (ArH) are depicted. At 100× magnification, the relative amounts of key intermediates can also be represented on the same scale.

A key observation is the change in mechanism early in the reaction, whereby the initial fast rate is replaced with a much slower, zero-order process. The rate of formation of the by-

[*] K. L. Vikse, Z. Ahmadi, C. C. Manning, Dr. D. A. Harrington, Dr. J. S. McIndoe
Department of Chemistry, University of Victoria
P.O. Box 3065, Victoria, BC, V8W 3V6 (Canada)
Fax: (+1) 250-721-7147
E-mail: mcindoe@uvic.ca

[**] K.L.V. thanks the University of Victoria for a Pacific Century Fellowship. J.S.M. thanks the CFI and BCKDF for infrastructure support; J.S.M. and D.A.H. thank the NSERC for operational funding (Discovery).

Supporting information for this article is available on the WWW under <http://dx.doi.org/10.1002/anie.201102630>.

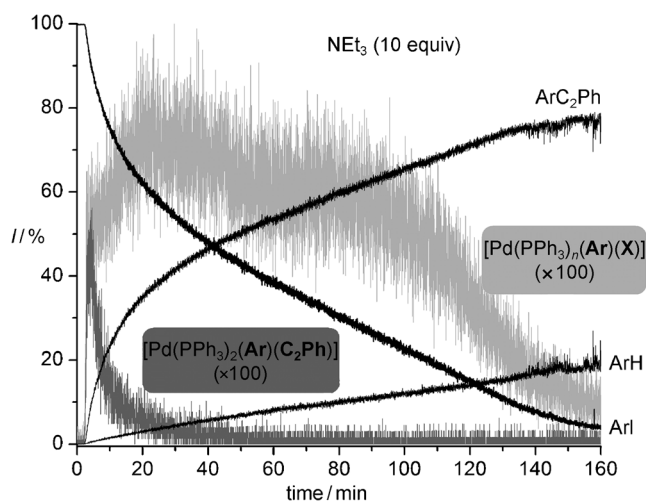
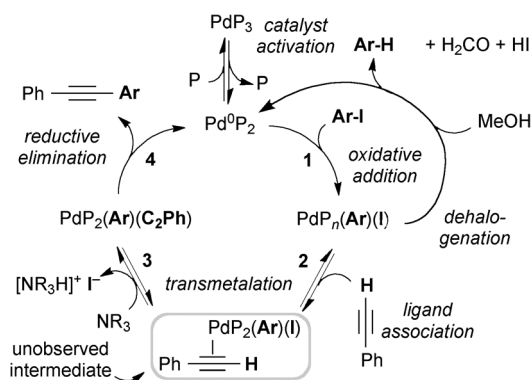


Figure 2. ESIMS intensity data over time for all key species containing $\text{Ar} = p\text{-C}_6\text{H}_4\text{CH}_2\text{PPh}_3^+$. The intensity has been multiplied by 100 for the palladium-containing intermediates.

product, ArH , through dehalogenation is essentially constant throughout (zero order). The changeover in mechanism corresponds to the beginning of the disappearance of $[\text{Pd}(\text{PPh}_3)_2(\text{Ar})(\text{C}_2\text{Ph})]$ ($\text{Ar} = p\text{-C}_6\text{H}_4\text{CH}_2\text{PPh}_3^+$). In contrast, $[\text{Pd}(\text{PPh}_3)_n(\text{Ar})(\text{X})]$ ($n = 1$ or 2 , $\text{X} = \text{halide}$, sum of all species) reaches a maximum concentration at the time of the mechanistic changeover, stays roughly constant, then diminishes to zero at the conclusion of the reaction. We suggest that the initial fast rate has reductive elimination as its rate-determining step, which accounts for the buildup of $[\text{Pd}(\text{PPh}_3)_2(\text{Ar})(\text{C}_2\text{Ph})]$. As this intermediate disappears, the steady state of $[\text{Pd}(\text{PPh}_3)_n(\text{Ar})(\text{X})]$ and zero-order kinetics now suggest that the transmetalation reaction becomes rate-determining (Scheme 1).

The buildup of either H^+ or I^- might affect the course of the reaction by driving step 3 backwards. To test this possibility, we added $[\text{NEt}_3\text{H}]\text{I}$ to the reaction mixture in a 1:1 ratio to the catalyst. The iodide had no effect on the progress of the reaction. $[\text{NEt}_3\text{H}]\text{I}$ was added instead, and the change in the reaction profile was dramatic (Figure 3).

The added H^+ entirely shuts down the initial fast rate of reaction, and the reaction proceeds under zero-order con-



Scheme 1. Catalytic cycle for the copper-free Sonogashira reaction. Only species containing Ar are visible by ESIMS; the intermediate in the gray box is speculative, as it was not observed during the reaction.

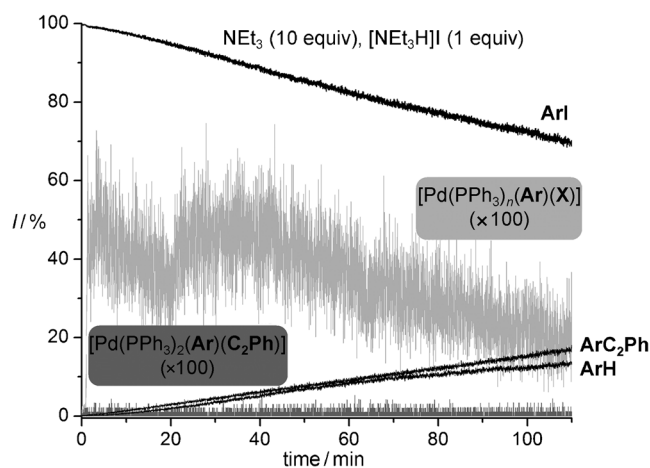


Figure 3. ESIMS intensity data over time for all key species containing $p\text{-C}_6\text{H}_4\text{CH}_2\text{PPh}_3^+$ in a reaction mixture to which $[\text{NEt}_3\text{H}]\text{I}$ (1 equiv) has been added. The intensity has been multiplied by 100 for the palladium-containing intermediates.

ditions throughout. $[\text{Pd}(\text{PPh}_3)_2(\text{Ar})(\text{C}_2\text{Ph})]$ is present only at very low levels, and the concentration of $[\text{Pd}(\text{PPh}_3)_n(\text{Ar})(\text{X})]$ is approximately steady-state. The overall slow rate of reaction means that the dehalogenation reaction has approximately the same rate as the coupling reaction. The fact that the dehalogenation is unaffected by the addition of protons suggests that the rate-determining step for this side reaction does not involve (de)protonation; a previous study on aryl chlorides suggests that the rate-determining step is the oxidative-addition step,^[26] but that assumption is unlikely to translate to the aryl iodide case.

For practical applications, a system in which the initial fast rate of reaction is preserved is desirable, and given that the presence of protons slows the reaction, a stronger base ought to more effectively sequester the proton and allow the reaction to continue operating in the faster regime. We repeated the reaction with DBU ($\text{p}K_{\text{a}} = 13.9$; $\text{p}K_{\text{a}}(\text{NEt}_3) = 9.0$). The fast first-order process dominated throughout the reaction (Figure 4), which was complete within 90 min. The yield was higher, and the product cleaner, because the dehalogenation side reaction could not compete as effectively with the desired coupling reaction. In this reaction, the amount of $[\text{Pd}(\text{PPh}_3)_2(\text{Ar})(\text{C}_2\text{Ph})]$ is high initially and drops off under first-order kinetics. Since the protonation step (step 3 in reverse) has been slowed because of the use of a stronger base, the reductive-elimination step remains rate-determining throughout.

We performed simulations of the reactions by making educated guesses about the relative rates of the many steps in the catalytic cycle. Optimization of the many independent parameters is nontrivial; however, our confidence in the cycle was solidified by a model that could not only predict the overall shape of all five traces in Figure 2, but that responded appropriately to changes in the initial conditions (added acid and stronger base) to accurately predict the behavior observed in Figures 3 and 4 (see the Supporting Information).

A direct comparison of the appearance of the product under the three different sets of reaction conditions (all

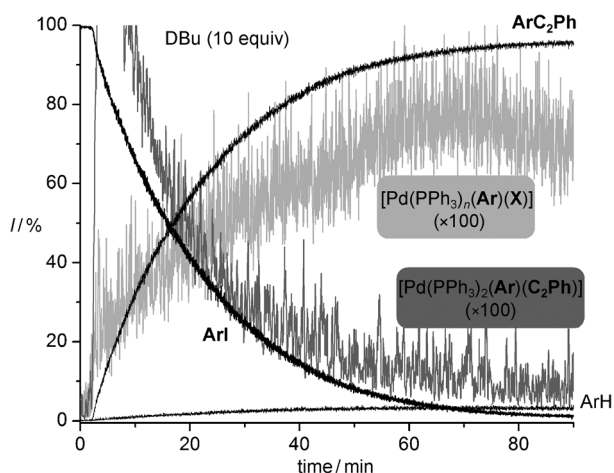


Figure 4. ESIMS intensity data over time for all key species containing $p\text{-C}_6\text{H}_4\text{CH}_2\text{PPh}_3^+$ in a reaction in which 1,8-diazabicyclo[5.4.0]undec-7-ene (DBU) has been used in place of NEt_3 . The intensity has been multiplied by 100 for the palladium-containing intermediates.

reactions were carried out on the same scale) is instructive (Figure 5), as the extent to which the addition of the acid compromises the reaction and the amount that the use of a stronger base improves the reaction become immediately evident. Understanding of the catalytic cycle is key to the improvement of reaction conditions in a rational fashion.

We are in the process of establishing the generality of our approach through its application to the full gamut of palladium-catalyzed cross-coupling reactions as well as many other catalytic reactions. We plan to develop methods to optimize our numerical modeling, but it is clear that even a qualitative picture based on the simultaneous tracking of substrates, products, and intermediates over time provides immediately useful insight into the nature of catalytic (or indeed, any) reactions. We anticipate that this method will

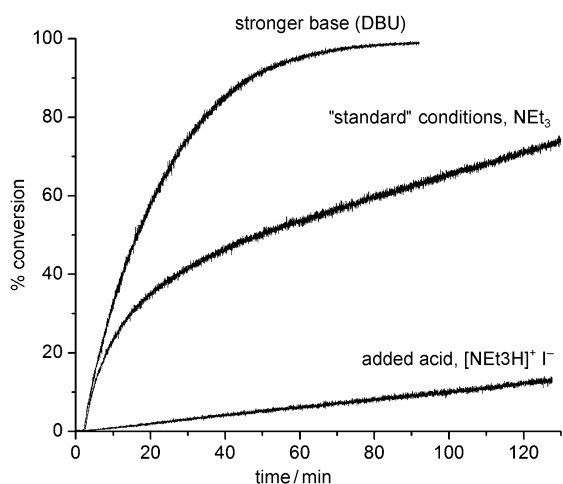


Figure 5. ESIMS intensity data over time for the appearance of $\text{IC}_6\text{H}_4\text{CH}_2\text{PPh}_3^+$ in the presence of different bases and added acid. The three reactions were carried out under otherwise identical conditions (same catalyst concentration, solvent, temperature, etc.).

become a versatile addition to the growing toolbox of spectroscopic^[28] and spectrometric^[29] techniques for the mechanistic analysis of catalytic and stoichiometric reactions.

Received: April 15, 2011
Published online: June 14, 2011

Keywords: electrospray ionization · homogeneous catalysis · mass spectrometry · reaction mechanisms · Sonogashira coupling

- [1] A. O. Aliprantis, J. W. Canary, *J. Am. Chem. Soc.* **1994**, *116*, 6985.
- [2] M. A. Aramendía, F. Lafont, M. Moreno-Mañas, R. Pleixats, A. Roglans, *J. Org. Chem.* **1999**, *64*, 3592.
- [3] J. M. Brown, K. K. Hii, *Angew. Chem.* **1996**, *108*, 679; *Angew. Chem. Int. Ed. Engl.* **1996**, *35*, 657.
- [4] C. Chevrin, J. Le Bras, F. Henin, J. Muzart, A. Pla-Quintana, A. Roglans, R. Pleixats, *Organometallics* **2004**, *23*, 4796.
- [5] P.-A. Enquist, P. Nilsson, P. Sjöberg, M. Larhed, *J. Org. Chem.* **2006**, *71*, 8779.
- [6] H. Guo, R. Qian, Y. Liao, S. Ma, Y. Guo, *J. Am. Chem. Soc.* **2005**, *127*, 13060.
- [7] C. Markert, M. Neuburger, K. Kulicke, M. Meuwly, A. Pfaltz, *Angew. Chem.* **2007**, *119*, 5996; *Angew. Chem. Int. Ed.* **2007**, *46*, 5892.
- [8] C. Raminelli, M. H. G. Precht, L. S. Santos, M. N. Eberlin, J. V. Comasseto, *Organometallics* **2004**, *23*, 3990.
- [9] A. A. Sabino, A. H. L. Machado, C. R. D. Correia, M. N. Eberlin, *Angew. Chem.* **2004**, *116*, 2568; *Angew. Chem. Int. Ed.* **2004**, *43*, 2514.
- [10] L. S. Santos, G. B. Rosso, R. A. Pilli, M. N. Eberlin, *J. Org. Chem.* **2007**, *72*, 5809.
- [11] A. Svennebring, P. J. R. Sjöberg, M. Larhed, P. Nilsson, *Tetrahedron* **2008**, *64*, 1808.
- [12] K. L. Vikse, M. A. Henderson, A. G. Oliver, J. S. McIndoe, *Chem. Commun.* **2010**, *46*, 7412.
- [13] J. Masllorens, I. González, A. Roglans, *Eur. J. Org. Chem.* **2007**, 158.
- [14] M. A. Schade, J. E. Fleckenstein, P. Knochel, K. Koszinowski, *J. Org. Chem.* **2010**, *75*, 6848.
- [15] R. Chinchilla, C. Nájera, *Chem. Rev.* **2007**, *107*, 874.
- [16] C. Amatore, A. Jutand, *Acc. Chem. Res.* **2000**, *33*, 314.
- [17] A. Jutand, S. Négri, A. Principaud, *Eur. J. Inorg. Chem.* **2005**, 631.
- [18] A. Tougerti, S. Negri, A. Jutand, *Chem. Eur. J.* **2007**, *13*, 666.
- [19] C. Amatore, S. Bensalem, S. Ghalem, A. Jutand, Y. Medjour, *Eur. J. Org. Chem.* **2004**, 366.
- [20] H. A. Dieck, F. R. Heck, *J. Organomet. Chem.* **1975**, *93*, 259.
- [21] C. Amatore, S. Bensalem, S. Ghalem, A. Jutand, *J. Organomet. Chem.* **2004**, *689*, 4642.
- [22] T. Ljungdahl, T. Bennur, A. Dallas, H. Emtenaes, J. Maartensson, *Organometallics* **2008**, *27*, 2490.
- [23] D. M. Chisholm, J. S. McIndoe, *Dalton Trans.* **2008**, 3933.
- [24] D. M. Chisholm, A. G. Oliver, J. S. McIndoe, *Dalton Trans.* **2010**, 39, 364.
- [25] C. Adlhart, P. Chen, *Helv. Chim. Acta* **2000**, *83*, 2192.
- [26] K. L. Vikse, M. P. Woods, J. S. McIndoe, *Organometallics* **2010**, *29*, 6615.
- [27] O. Navarro, H. Kaur, P. Mahjoor, S. P. Nolan, *J. Org. Chem.* **2004**, *69*, 3173.
- [28] S. Monfette, J. M. Blacquiere, D. E. Fogg, *Organometallics* **2011**, *30*, 36.
- [29] V. G. Santos, T. Regiani, F. F. G. Dias, W. Romão, J. L. Paz Jara, C. F. Klitzke, F. Coelho, M. N. Eberlin, *Anal. Chem.* **2011**, *83*, 1375.